

Relaxor ferroelectric behavior of “A” site deficient Bismuth doped Barium Titanate ceramic

T. Badapanda · V. Senthil · D. K. Rana · S. Panigrahi · S. Anwar

Received: 21 March 2012 / Accepted: 30 July 2012 / Published online: 14 August 2012
© Springer Science+Business Media, LLC 2012

Abstract A site deficient Bi doped BaTiO₃ ceramic with general formula Ba_{1-x}Bi_{2x/3}TiO₃ ($x=0.00, 0.01, 0.025$) is prepared by solid state reaction route. The phase formation and structural property of all compositions are studied by X-Ray Diffraction pattern. The pattern reports single phase tetragonal crystal system with space group of *P4mm*. The XRD study also reveals that bismuth (Bi) replaces “A” site (Ba) of the BaTiO₃ perovskite. The surface morphology of the sintered pellets is studied by scanning electron microscopy which shows a decrease in grain size with an increase in Bi concentration. The temperature and frequency dependent dielectric behaviors of the compositions are studied to show the effect of Bi ion on the “A” (Ba) site of BaTiO₃ perovskite. The dielectric constant decreases and transition temperature increases with increase in Bi concentration. Substitution of Bi ion induces diffuse ferroelectric behavior and the degree of diffuseness increases with increase in doping concentration. The ferroelectric behavior is also confirmed by the P-E loop study.

Keywords X-Ray diffraction · Relaxor ferroelectrics · Diffuse phase transition · P-E loop

T. Badapanda (✉)
Department of Physics, C. V. Raman College of Engineering,
Bhubaneswar 752054, Odisha, India
e-mail: badapanda.tanmaya@gmail.com

V. Senthil · D. K. Rana · S. Panigrahi
Department of Physics, National Institute of Technology,
Rourkela 769008, Odisha, India

S. Anwar
Colloids & Materials Chemistry,
Institute of Minerals and Materials Technology,
Bhubaneswar 751013, Odisha, India

1 Introduction

Relaxor ferroelectric materials with complex perovskite structure have been studied extensively due to its wide use in the fabrication of multilayer ceramic capacitors, electrostrictive actuators, and electromechanical transducers. Most relaxor ferroelectrics belong to the family of complex lead-based perovskite oxides, such as such as PMN–PT, PNN–PZT, PLZT, etc. which is often considered as a model system and has been widely studied due to its excellent ferroelectric, dielectric and piezoelectric properties [1–3]. In particular, lead based solid solutions have dominated for decades the technological field responsible for the development of piezoelectric materials [4]. However these compositions have the obvious disadvantage of volatility and toxicity of lead. Therefore much effort has been made towards investigating environment-friendly ‘lead-free’ relaxor materials [5]. Thus, the scientific community has searched new materials with interesting chemical and physical properties in order to replace the Pb-based compounds for environmental friendly applications [6]. There are many lead-free materials with perovskite structure such as BaTiO₃ (BT), (Bi_{1/2}Na_{1/2})TiO₃ (BNT), (Bi_{1/2}K_{1/2})TiO₃ (BKT) and KNbO₃ (KN) have been investigated [7, 8] in terms of their dielectric relaxation, ferroelectric phase transition and electrical properties. Out of those, the BaTiO₃-based ceramics have been widely investigated. The reason for the interest is primarily two fold; firstly, BaTiO₃-based materials offer a wide range of commercial applications and secondly, BaTiO₃ is often perceived as a ‘model’ (non-lead based) ferroelectric perovskite-type oxide (ABO₃) that exhibits several polymorphic phase transitions and is therefore used to correlate important dielectric/ferroelectric properties such as variations in polymorphic phase transition temperatures,

permittivity and dielectric loss with chemical doping and ceramic microstructure.

The study of the electrical properties of BaTiO₃ had been and still is a very important research topic because of its technical importance and the difficulty of explaining the behavior thoroughly. The electrical resistance and ferroelectric transition temperature can be controlled effectively by doping in either barium or titanium site with proper donor impurity ions [9–11]. Barium titanate and its related compounds have been widely used in the manufacture of ceramic multilayer capacitors and PTC resistors. Since its discovery, BaTiO₃ has been used as a high permittivity capacitor material because of its high dielectric constant [12]. Variation in chemical composition or thermal treatment in these ceramics led to quite drastic changes in physical properties while retaining substantially piezoelectric properties [13]. So to trigger the coexistence between order (ferroelectric) and disorder (relaxor), we decided to add another degree of freedom by introducing a disorder on the A site (Ba²⁺) in BaTiO₃ ceramic. This can be achieved with the heterovalent substitution of Ba²⁺ cation with Bi³⁺. The choice of Bi³⁺ (substituted for Ba²⁺) cation is due to its 6sp² lone pair (like Pb²⁺) and such an electronic environment is favorable for the relaxor effect without the disadvantage of lead pollution [14]. Bismuth is also used as a donor dopant for BaTiO₃-based PTC (positive temperature coefficient) Thermistors [15] and was also found to be able to enhance the magnitude of the positive coefficients of resistance [16]. In this paper we have studied the effect of vacancy to on the structural, microstructural, dielectric and ferroelectric property of heterovalent ion (Bi) substitution on the “A” site of BaTiO₃ perovskite.

2 Experimental techniques

The stoichiometric ratio of starting chemicals BaCO₃ (99.9 %), TiO₂ (99.9 %) and Bi₂O₃ (99.9 %) (E. Merck India Ltd.) were weighed for the composition Ba_{1-x}Bi_{2x/3}TiO₃ (x=0.0–0.025). The weighed powders were ball milled by a laboratory ball milling machine for 8 h using high purity Zirconia balls and acetone as a medium. After drying, calcination was done in a high purity alumina crucible at 1,200 °C for 4 h in a conventional programmable furnace. The calcined powders were grinded by agate mortar and then pressed into disc form at a pressure 250 MPa using a hydraulic press with 5 wt.% PVA solution added as binder. The discs were sintered at 1,300 °C for 4 h with 5 °C min⁻¹ heating rate. The phase purity of the calcined powders was confirmed by the X-Ray Diffractometer. X-ray Diffractometer analysis of the samples was carried out using a Philips diffractometer model PW-1830 with Cu-K_α (λ=1.5418 Å)

radiation in a wide range of 2θ (20° < 2θ < 70°) at a scanning rate of 1/2° min⁻¹. Density and microstructure information was obtained by the Archimedes principle and Scanning Electron Microscope (JEOL T-330) respectively. For electrical measurements, silver electrodes were applied on the opposite disk faces and were heated at 700 °C for 5 min. The frequency (1KHz-1 MHz) and temperature (30–200 °C) dependent dielectric measurement were carried out using a Hioki LCR meter (model 3532–50) connected to PC. The ferroelectric hysteresis loop measurement was performed in a P-E loop tracer (Radiant Technologies) based on modified Sawyer-Tower circuit.

3 Result and discussions

3.1 X-ray diffraction

Fig. 1 shows the XRD pattern of the Bi doped BaTiO₃ and all the peaks in the patterns are well matched with JCPDS 05-0626. The XRD peak shows purely tetragonal single phase crystal related to the tetragonal system with space group of P4mm. No evidence of the precursor phase BaCO₃, TiO₂ or Bi₂O₃ is detected by XRD pattern. A careful analysis of the XRD pattern confirms that peaks are shifted towards a higher 2θ angle. It is also observed that Bi replaced the A-site of a perovskite lattice. The same result has also been reported by Zhou et al. [17]. Figure 2 shows the lattice parameter, tetragonality and unit cell volume of Ba_{1-x}Bi_{2x/3}TiO₃ ceramics. These data are estimated through the CHEKCELL program using the regression diagnostics combined with nonlinear least squares. It is observed that the lattice parameter and the tetragonality increase with increase in Bi content. In an ideal cubic perovskite ABO₃ structure, the coordination of the A-site is 12. The ionic radius of 12-coordinated Bi³⁺ is 0.145 nm [18], which is

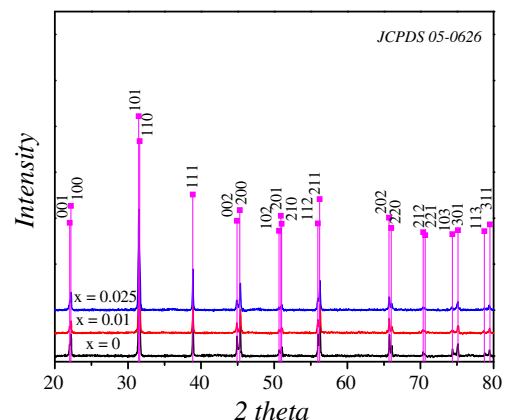
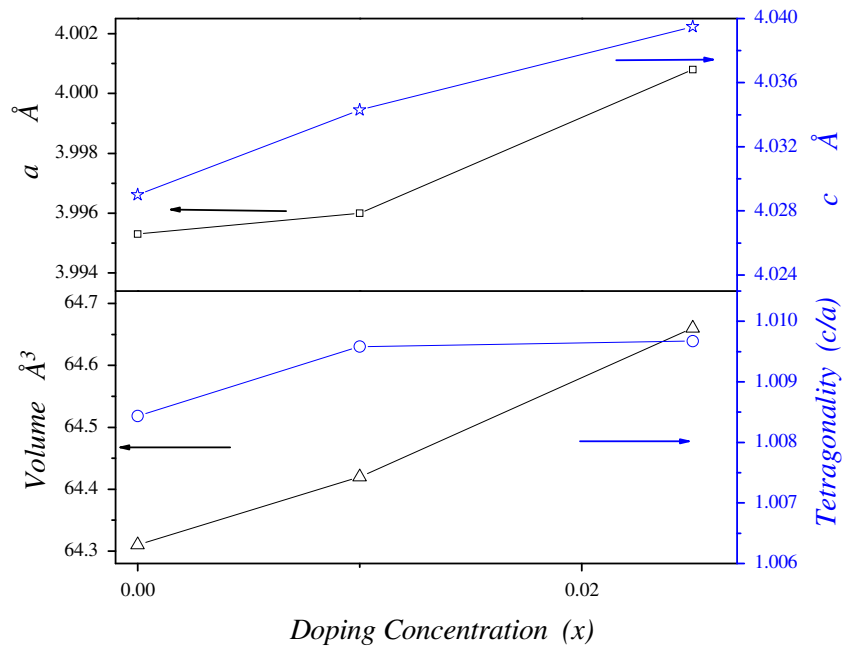
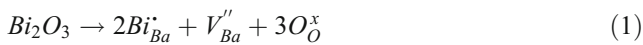


Fig. 1 XRD patterns of Ba_{1-x}Bi_{2x/3}TiO₃ (0 ≤ x ≤ 0.025) ceramic calcined powders at 1,200 °C for 4 h

Fig. 2 Lattice parameters, Volume and Tetragonality of $Ba_{1-x}Bi_{2x/3}TiO_3$ ($0 \leq x \leq 0.025$) ceramics



nearly comparable to the value of 0.16 nm for Ba^{2+} . Therefore, the substitution of Bi^{3+} for Ba^{2+} will take place, according to the Kroger-Vink notation, as follows:



where Bi and Ba stands for a bismuth atom on barium site with one positive charge, $V_{Ba}^{\prime\prime}$ for a barium vacancy with two negative charges and O_O^x for a neutral oxygen atom on an oxygen site. Thus, the addition of Bi_2O_3 in the $BaTiO_3$ -based ceramics leads to the formation of barium vacancy by a charge compensation mechanism.

3.2 Microstructure and elemental analysis

Figure 3 shows the scanning electron microscope (SEM) images of Bi modified $BaTiO_3$ samples sintered at 1,300 °C for 4 h which shows well-developed growth grains with significant reduction in grain size. The grain size is ~10 μm, 2 μm and 1 μm for $x=0.0, 0.01$ and 0.025 respectively. The possible reason for decreasing the grain size is that more crystal nucleus was formed with increase in Bi content. It is well known that $BaTiO_3$ doped with small amount of donor impurities yields cation vacancy compensation and results in the material being fine-grained [19, 20]. The densities of all the samples are measured by Archimedes method using distilled water as a medium and found to be 97 %, 92 % and 89 % of the theoretical density for $x=0.0, 0.01, 0.025$ respectively. Figure 3 shows the elemental analysis of Bi substituted $BaTiO_3$ ceramic which shows that all compositions maintained their stoichiometry after sintering. Non-volatility of Bismuth in the high temperature sintered pellets may be

due to the complete incorporation of Bi inside the distorted $BaTiO_3$ perovskite.

3.3 Dielectric study

The temperature dependence of dielectric constant (ϵ') and dissipation factor ($\tan \delta$) for the $Ba_{1-x}Bi_{2x/3}TiO_3$ samples at 1 kHz, 10 kHz, 100 kHz and 1 MHz is shown in Fig. 4(a–c). The temperature dependence of the dielectric permittivity at different frequencies shows that for undoped $BaTiO_3$ sample there exists a sharp dielectric peak where as a frequency dispersion around the dielectric peak and diffuse phase transition behavior is observed for Bi doped samples. The degree of diffuseness increases with increase in Bi concentration in $Ba_{1-x}Bi_{2x/3}TiO_3$ ceramic. There is also frequency dispersion at around Curie temperature in the dielectric loss curve which indicates that the dielectric loss is more sensitive to a small distortion which indicates appearance of polar micro-regions in the samples [21, 22]. The dielectric constant as a function of temperature at constant frequency of 100 kHz is tabulated in Table 1.

It is well known that the classical ferroelectrics follow the Curie–Weiss law above Curie temperature and is expressed by the following relationship,

$$\frac{1}{\epsilon} = \frac{(T - T_o)}{C} \quad (at T > T_c) \quad (2)$$

Where T_o is the Curie temperature and C is the Curie–Weiss constant. The occurrence of deviation has been attributed to short-range correlation between the nano-polar domains [23]. Table 1 shows the fitting parameter at 100 kHz for all the samples. It is seen that the dielectric constant of $Ba_{1-x}Bi_{2x/3}TiO_3$ ceramics follows the Curie–Weiss

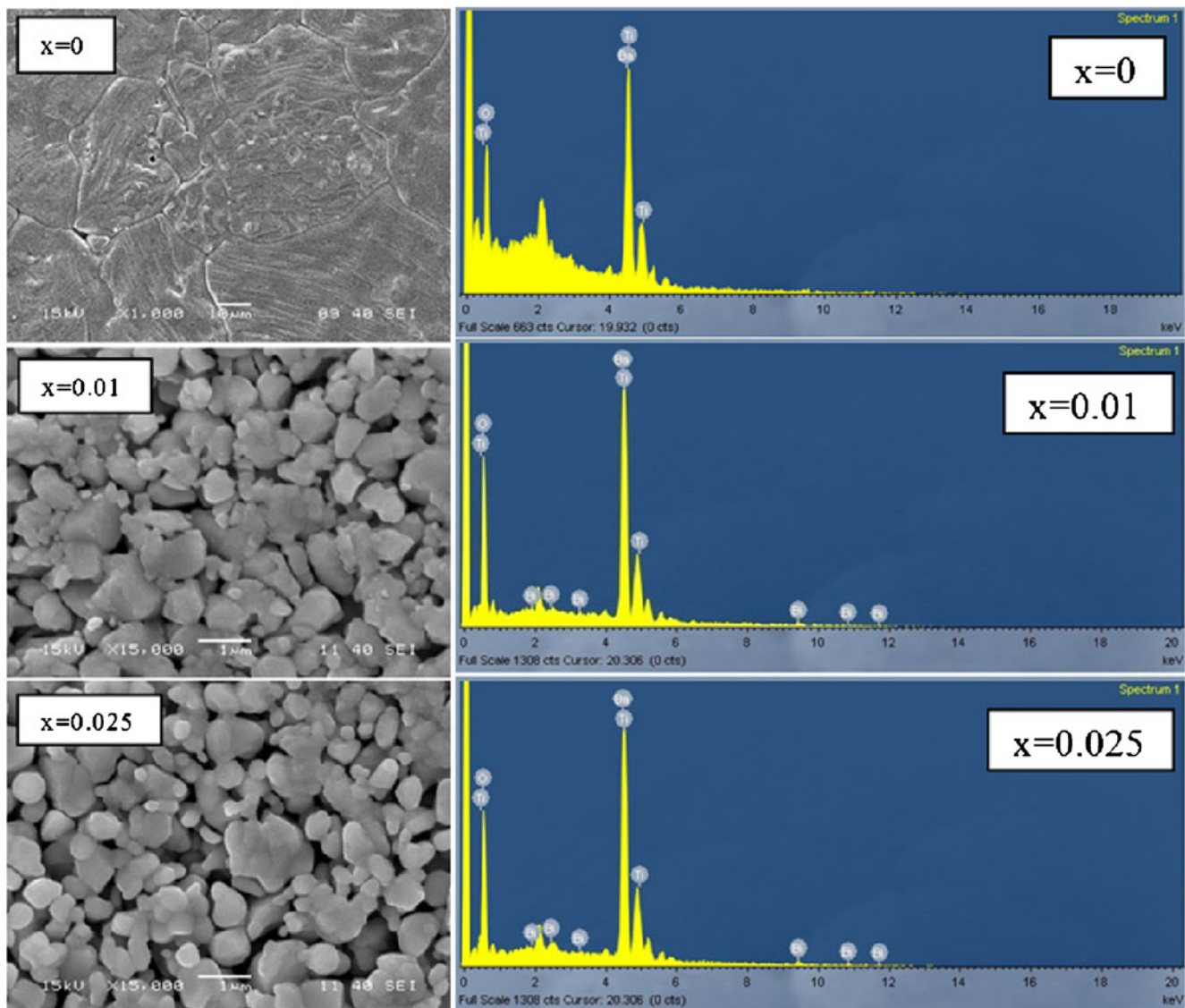


Fig. 3 Scanning electron microscopy images (SEM) and Elemental analysis (EDX) of sintered pellet of $\text{Ba}_{1-x}\text{Bi}_{2x/3}\text{TiO}_3$ ($0 \leq x \leq 0.025$) ceramics at $1,300^\circ\text{C}$ for 4 h

law at temperature much higher than the T_m . An empirical parameter ΔT_m , defined as $\Delta T_m = T_{\text{dev}} - T_m$, is often used as a measure of the degree of deviation from the Curie–Weiss law. Here, T_{dev} is the temperature at which dielectric permittivity starts to deviate from Curie–Weiss law.

Uchino and Nomura [24] modified the Curie–Weiss law for the diffuseness phase transition and given as;

$$\frac{1}{\varepsilon} - \frac{1}{\varepsilon_m} = \frac{(T - T_m)^\gamma}{C_1} \quad (\text{at } T > T_m) \quad (3)$$

where γ and C_1 are modified constants, with $1 < \gamma < 2$. The value of the parameter γ gives information about the character of the phase transition. Its limiting values are $\gamma = 1$ and $\gamma = 2$. The value of γ is 1 for the case of a normal

ferroelectric and $\gamma = 2$ (quadratic) is valid for an ideal ferroelectric relaxor [25–27]. A plot of $\ln(1/\varepsilon - 1/\varepsilon_m)$ as a function of $\ln(T - T_m)$ is shown in Fig. 5 for $\text{Ba}_{1-x}\text{Bi}_{2x/3}\text{TiO}_3$ samples. By fitting with Eq. (3), the exponent γ , determining the degree of the diffuseness of the phase transition, is obtained from the slope of the $\ln(1/\varepsilon - 1/\varepsilon_m)$ vs $\ln(T - T_m)$ plot which is shown in Table 1.

The diffuseness of the phase transition can be described by an empirical parameter ΔT_{diff} , defined as

$$\Delta T_{\text{diff}} = T_{0.9\varepsilon_m(100\text{Hz})} - T_{\varepsilon_m(100\text{Hz})} \quad (4)$$

i.e. the difference between $T_{0.9\varepsilon_m(100\text{Hz})}$ (the temperature corresponding to 90 % of the maximum of the dielectric constant (ε_m) at higher temperature side) and $T_{\varepsilon_m(100\text{Hz})}$ (T_{ε_m} at 100 Hz)). The value of ΔT_{diff} shows the more

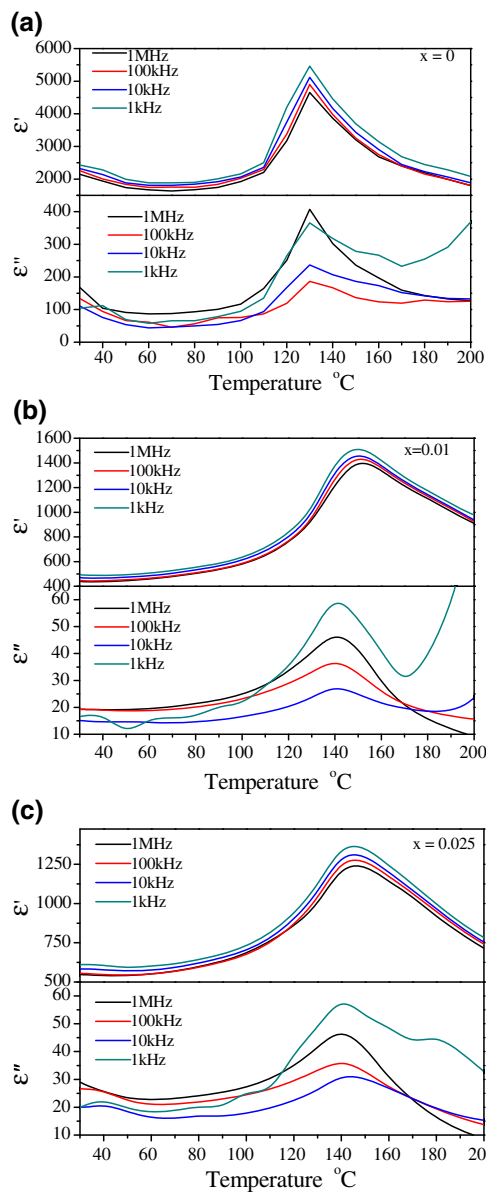


Fig. 4 Temperature dependency of dielectric constant (ϵ') and loss tangent ($\tan \delta$) of $\text{Ba}_{1-x}\text{Bi}_{2x/3}\text{TiO}_3$ ceramics (a) $x=0$, (b) $x=0.01$, (c) $x=0.025$

diffusive nature of doped BaTiO_3 ceramics as compared to undoped one. The frequency dispersion near dielectric maxima in ferroelectrics has been attributed to the distribution of relaxation times. A large number of theoretical

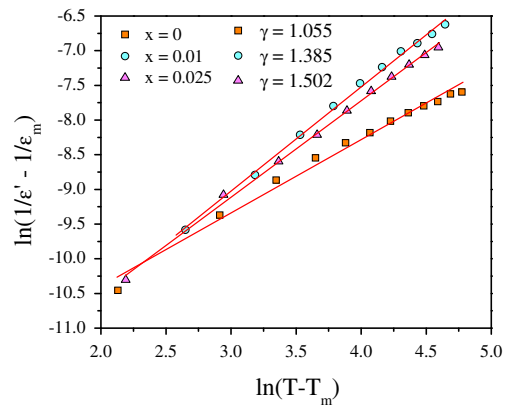


Fig. 5 $\ln(1/\epsilon' - 1/\epsilon_m)$ vs. $\ln(T - T_m)$ of $\text{Ba}_{1-x}\text{Bi}_{2x/3}\text{TiO}_3$ ($0 \leq x \leq 0.025$) at 100 kHz

models have been proposed to understand the diffusiveness of the dispersion. [28]. The normalized dielectric constant as a function of normalized temperature for $\text{Ba}_{1-x}\text{Bi}_{2x/3}\text{TiO}_3$ is shown in Fig. 6. These figures facilitate the observation of the extent of diffuseness of compositions exhibiting different values of T_{max} . The area under the curve represents the extent of diffuseness. Increment in the area under the normalized curve confirms the extent of diffusiveness by increasing Bi^{3+} content and also agreed well with the Uchino and Nomura’s modified Curie–Weiss law (Eq. 3).

All compositions exhibit a broad permittivity maximum with temperature. The broadness increases with increasing substitution rate. Peak broadening may be quantified by the parameter δ , which is related with permittivity and temperature as follows [29]

$$\frac{1}{\epsilon'} - \frac{1}{\epsilon'_m} = \frac{(T - T_m)^2}{2\epsilon_m \delta^2} \tag{5}$$

δ parameters of different compositions are calculated by fitting permittivity-temperature data as shown in Fig. 7 and the fitting values are presented in Table 1. The broadening increases significantly with Bi^{3+} substitution. It is well accepted that the broadness in the ferroelectric material originates from the compositional fluctuation and disorder in crystallographic sites when one or more cations occupy the same site in the structure

Table 1 Parameters obtained from temperature dependency dielectric study on the composition $\text{Ba}_{1-x}\text{Bi}_{2x/3}\text{TiO}_3$ ($0 \leq x \leq 0.025$) ceramic at 100 kHz

Composition	ϵ_m	T_m (°C)	T_o (°C)	$C \times 10^5$	γ	δ	ΔT_m (°C)	ΔT_{dif} (°C)
$x=0.0$	4,512	131	94	1.869	1.055	139	5	5
$x=0.01$	1,274	146	110	0.661	1.385	108	34	33
$x=0.025$	1,430	151	107	0.865	1.502	106	38	39

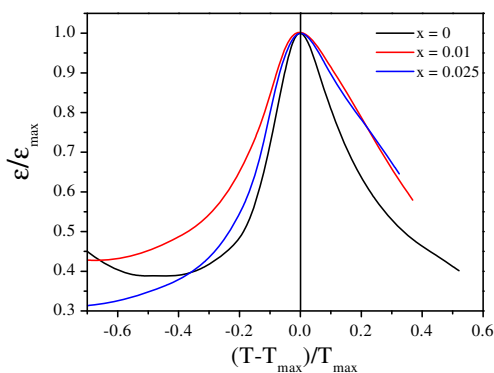


Fig. 6 Normalized dielectric constant of $Ba_{1-x}Bi_{2x/3}TiO_3$ ($0 \leq x \leq 0.025$) ceramics at 100 kHz

[30]. The value of δ , which is related to the broadening of the $\epsilon(T)$ curve, can be used to determine the degree of compositional fluctuations in the material. This diffuseness parameter δ_g depends upon not only the chemical composition of the material but also on the frequency of the electric field [31, 32].

The diffuse phase transition behavior as observed in this ceramic can be induced by many reasons, such as microscopic composition fluctuation, the merging of micropolar regions into macropolar regions, or a coupling of order parameter and local disorder mode through the local strain. Vugmeister and Glinchuk reported that the randomly distributed electrical strain field in a mixed oxide system is the main reason leading to the diffuse behavior [33]. As no macroscopic phase separation exists in the studied ceramic, we cannot exclude chemical heterogeneity in nanoscale. The distortion arising in the oxygen octahedra, a redistribution of the charge, and local formation of charge center result may be the sources of random field. This kind of random field is much weaker than that stemming from heterovalent cation substitution as in conventional ferroelectrics. Hence, at high temperature, the strength of random field-fluctuating dipole

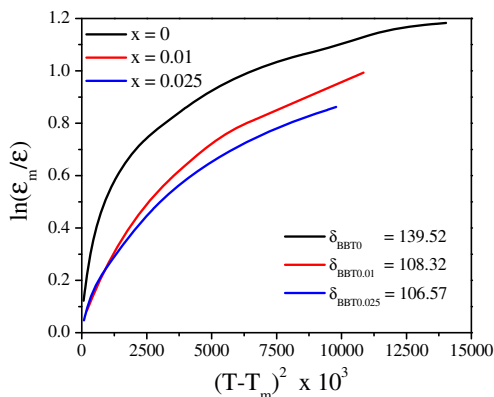


Fig. 7 $(T-T_m)^2$ vs. $\ln(\epsilon_m/\epsilon)$ of $Ba_{1-x}Bi_{2x/3}TiO_3$ ($0 \leq x \leq 0.025$) at 100 kHz

moments of the individual unit cell can give rise to polar nanoregions. Here the polar correlations are strongly diminished and polar domains are less likely to nucleate. The bismuth substitution not only decreases the grain size, but also the size and distribution of the polar-regions. This can lead to the broadening of relaxation time and significant improvement of the diffuse properties of Bi-doped $BaTiO_3$ ceramics.

In perovskite type compounds, the relaxor behavior appears when at least two cations occupy the same crystallographic site A or B. In our composition, the Bi^{3+} atom occupies the A site and makes vacancy because of its higher valency than the actual A site atom (Ba^{2+}). Due to this, the higher valency creates disorder in the complete site of the $BaTiO_3$ ceramic and creates the frequency and temperature dependence dielectric constant and its called as relaxor behavior. In relaxor materials, an empirical Vogel–Fulcher (VF) relationship can be used to account for the dielectric relaxation nature [34]. The dielectric relaxation appears as a result from thermally activated polarization reversals between two equivalent variants. Based on this model, the polarization flipping frequency ν_o is related to the activation energy E_a (the barrier between two equivalent polarization states) as follows:

$$\nu = \nu_o \exp \left[\frac{-E_a}{k_B(T_m - T_f)} \right] \tag{6}$$

where ν_o is the attempt frequency of dipole reorientation, E_a is the activation energy (i.e., the energy barrier between two equivalent polarization states), k_B is Boltzmann’s constant, and T_f is the static freezing temperature (i.e., the temperature at which dynamic reorientation of the dipolar cluster polarization can no longer be thermally activated). Figure 8

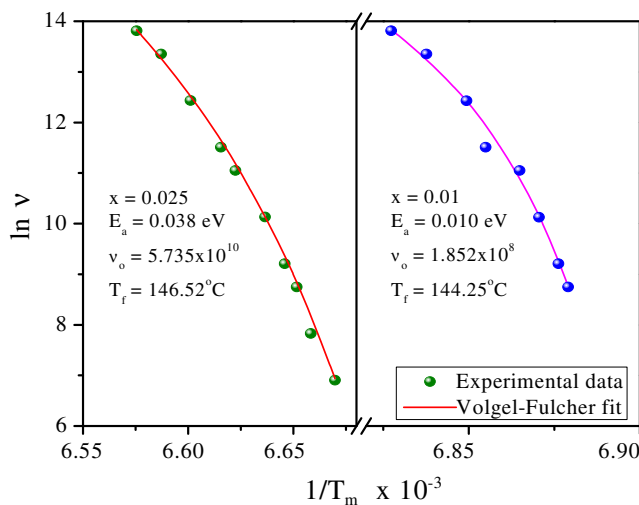


Fig. 8 Volgel-Fulcher fitting for $Ba_{1-x}Bi_{2x/3}TiO_3$ with different Bi($x=0.01, 0.025$) content

Table 2 Parameters obtained from the fitting of Eq. (6) on the composition $Ba_{1-x}Bi_{2x/3}TiO_3$ ($0 \leq x \leq 0.025$) ceramic

Composition	T_f (°C)	ν_0 (Hz)	E_a (eV)
$x=0.01$	144.25	1.852×10^8	0.01
$x=0.025$	146.52	5.73×10^{10}	0.038

shows the temperature dependence of the relaxation frequency, plotted as $1/T_m$ vs $\ln \nu$, and the best fit of equation to the experimental data. The fitting parameters of the VF model are tabulated in Table 2, which provides the evidence of the relaxor behavior in Bi^{3+} substituted $BaTiO_3$ ceramic.

The relaxor ferroelectric phase transition in ($BaTiO_3$) ceramics can also be explained by the substitution of Ba^{2+} by Bi^{3+} ions into the A-site. For every two Bi^{3+} substituting ions (Bi_{Ba}^{3+}) only one A-site vacancy (V_{Ba}'') is created, which produces compositional fluctuation on a microscopic scale. In the same way, the presence of Bi^{3+} ions in the A-site and their interaction with A-site vacancies give rise to a lattice distortion. This lattice distortion and the compositional fluctuation originating from Bi_{Ba}^{3+} and V_{Ba}'' inclusions in the $BaTiO_3$ structure may explain the diffusion of ferroelectric phase transition and relaxor ferroelectric behaviour observed for these compounds [35, 36]. The Bi^{3+} ion substitutions for Ba^{2+} in BT ceramics could also be located at off-centred positions and A-site vacancies (V_{Ba}'') might also appear to compensate the charge imbalance arising from substitution of the A-site by Bi^{3+} ions. A random electric field formed by off-centred Bi^{3+} ions and Bi^{3+} -(V_{Ba}'') dipoles would then suppress the ferroelectricity of $BaTiO_3$ solid solutions, resulting in the diffuse behaviour of the Bi-doped $BaTiO_3$ system. Again, Bi_{Ba}^{3+} and V_{Ba}'' increase with the increase of Bi^{3+} , and for this reason the compositional

Table 3 Parameters obtained from P-E loop of $Ba_{1-x}Bi_{2x/3}TiO_3$ ($0 \leq x \leq 0.025$) ceramic

Composition	P_{max} ($\mu C/cm^2$)	P_r ($\mu C/cm^2$)	E_c (kV/cm)
$x=0^*$	12.823	3.019	2.452
$x=0.01^{**}$	5.45	2.069	7.821
$x=0.025^{**}$	5.421	1.536	4.785

*max field=15 kV/cm, **max field=30 kV/cm

inhomogeneity is enhanced. As a consequence, increase of Bi content enlarges the degree of diffuseness as observed experimentally.

3.4 Ferroelectric polarization versus electric field study

Figure 9 shows the ferroelectric hysteresis loop of Bi doped $BaTiO_3$ ceramics obtained under a maximum applied electric field of 15 kV cm^{-1} of undoped $BaTiO_3$ and 30 kV cm^{-1} of the doped samples. The breakdown of the undoped $BaTiO_3$ ceramic (at 19 kV cm^{-1}) is very faster than the doped one. The P-E loop for all the compositions are recorded at room temperature and at a frequency of 100 Hz. The values of remnant polarization (P_r) and coercive field (E_c) are listed in Table 3. It can be seen that coercive field (E_c) and remnant polarization (P_r) decrease with increase in bismuth content. The decrease in coercive field indicates that the material gets soft. For doped samples; the decrease in P_r may be due to the increase in concentration of oxygen vacancies in the system as a result, the domain pinning effect gets increased. The decrease in P_r is also due to presence of pores in addition to the decrease in grain size.

4 Conclusions

$Ba_{1-x}Bi_{2x/3}TiO_3$ ceramic compositions are prepared by the conventional solid-state reaction route. The XRD shows a single phase tetragonal system with space group of $P4mm$. The temperature and frequency dependency dielectric study shows that Bi_2O_3 incorporation induced the diffuse phase transition and relaxor ferroelectric behaviour in the $BaTiO_3$ system. The diffuseness of the phase transition behaviour is enhanced with an increase in Bi content. The transition temperature of $Ba_{1-x}Bi_{2x/3}TiO_3$ ceramic shifted remarkably to a higher temperature with Bi^{3+} content. The dielectric relaxations show a sufficiently good fit with the Vogel–Fulcher relationship. The ferroelectric behavior is studied by hysteresis loop. The remnant polarization shows a slight decrease with the substitution level.

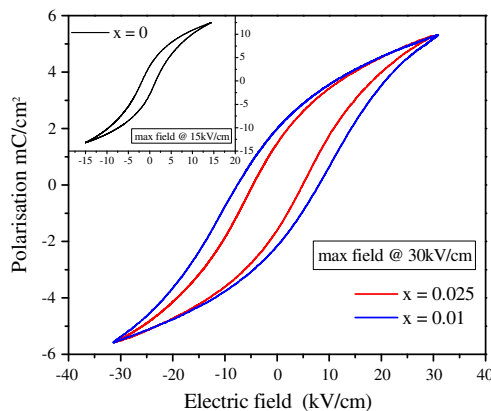


Fig. 9 Polarisation vs. Electric field loop of $Ba_{1-x}Bi_{2x/3}TiO_3$ ($0 \leq x \leq 0.025$) ceramic at room temperature

Acknowledgements The authors thank the Prof. P. Kumar and research groups for provide their instrumental facilities to carry out the research works.

References

1. W. Chaisan, R. Yimmirun, S. Ananta, D.P. Cann, *Mater. Lett.* **59**, 3732 (2005)
2. M. Adamczyk, M. Adamczyk, Z. Ujma, L. Szymczak, A. Soszynski, Koperski, *J. Mater. Sci. Eng. B* **136**, 170 (2007)
3. P. Kumar, S. Singh, J.K. Juneja, C. Prakash, K.K. Raina, *Physica B* **404**, 1752 (2009)
4. H. Fu, R.E. Cohen, *Nature* **403**, 281 (2000)
5. T. Maiti, R. Guo, A. S. Bhalla, *J. Am. Ceram. Soc.* 911769 (2008)
6. X. Wang, Y. Yang, *J. Phys. D* **42**, 075419 (2009)
7. J. Ravez, A. Simon, *J. Solid State Chem.* **162**, 260 (2001)
8. T. Takennaka, H. Nagata, Y. Hirume, V. Yoshii, K. Matumono, *J. Electroceram.* **19**, 259 (2007)
9. V.J. Tennery, R.L. Cook, *J. Am. Ceram. Soc.* **44**, 187 (1961)
10. T. Murakami, T. Miyashita, M. Naakahara, E. Sekine, *J. Am. Ceram. Soc.* **56**, 294 (1973)
11. G. Arlt, D. Hennings, G. de With, *J. Appl. Phys.* **58**, 1619 (1985)
12. G. Fagen James, *Am. Ceram. Soc. Bull.* **72**, 69 (1993)
13. S.B. Desu, D.A. Payne, *J. Am. Ceram. Soc.* **73**, 3391 (1990)
14. A. Simon, J. Ravez, M. Maglione, *Solid State Sci.* **7**, 925 (2005)
15. O. Saburi, *J. Phys. Soc. Jpn.* **14**, 1159 (1959)
16. P. Padmini, T.R.N. Kutty, *J. Mater. Sci.: Mater. Electron.* **5**, 203 (1994)
17. L. Zhou, P.M. Vilarinho, J.L. Baptista, *J. Am. Ceram. Soc.* **82**, 1064 (1999)
18. T. Okawa, M. Imaeda, H. Ohsato, *Mater. Sci.Eng. B* **88**, 58 (2002)
19. J. Nowotny, *Science of Ceramic Interfaces II* (Elsevier, Amsterdam, 1994), p. 1
20. H.T. Kim, Y.H. Han, *Ceramics International* **30**, 1719 (2004)
21. C. Ang, J.F. Scott, Z. Yu, H. Ledbetter, J.L. Baptista, *Phys. Rev. B* **59**, 6661 (1999)
22. C. Ang, Z. Yu, P. Lunckemer, A. Loidl, *Phys. Rev. B* **59**, 6665 (1999)
23. D. Viehland, S.J. Jang, L.E. Cross, M. Wuttig, *Phys. Rev. B* **46**, 8003 (1992)
24. K. Uchino, S. Nomura, *Integr. Ferroelectr* **44**, 55 (1982)
25. G.A. Smolenski, A.L. Agranovskaya, *Sov. Phys. Tech. Phys.* **3**, 1380 (1958)
26. C. Ang, Z. Jing, Z. Yu, *J. Phys. Condens. Matter* **14**, 8901 (2002)
27. P. Victor, R. Ranjith, S.B. Krupanidhi, *J. Appl. Phys.* **94**, 7702 (2003)
28. G. Fulcher, *J. Am. Ceram. Soc.* **8**, 339 (1925)
29. V.V. Kirillov, V.A. Isupov, *Ferroelectrics* **5**, 3 (1973)
30. J. Tellier, P.H. Boullay, M. Manier, D. Mercurio, *J. Solid State Chem.* **177**, 1829 (2004)
31. S. Miga, K. Wojcik, *Ferroelectrics* **100**, 167 (1989)
32. S.M. Pilgrim, A.E. Sutherland, S.R. Winzer, *J. Am. Ceram. Soc.* **73**, 3122 (1990)
33. B.E. Vugmeister, M.D. Glinchuk, *Rev. Mod. Phys.* **62**, 993 (1990)
34. U. Weber, G. Greuel, U. Boettger, S. Weber, D. Hennings, R. Waser, *J. Am. Ceram. Soc.* **84**, 759 (2001)
35. X. Chou, J. Zhai, H. Jiang, X. Yao, *J. Appl. Phys.* **102**, 084106 (2007)
36. D.Y. Lu, M. Toda, M. Sugano, *J. Am. Ceram. Soc.* **89**, 3112 (2006)